Title

Expansion of immunoglobulin-secreting cells and defects in B cell tolerance in Rag-dependent immunodeficiency

Journal

Journal of Experimental Medicine, 207(7)

ISSN

0022-1007

Authors

Walter, Jolan E
Rucci, Francesca
Patrizi, Laura
et al.

Publication Date

2010-07-05

DOI

10.1084/jem.20091927

Peer reviewed

Expansion of immunoglobulin-secreting cells and defects in B cell tolerance in *Rag*-dependent immunodeficiency

Jolan E. Walter,[1] Francesca Rucci,[1] Laura Patrizi,[1] Mike Recher,[1] Stephan Regenass,[4] Tiziana Paganini,[5] Marton Keszei,[2] Itai Pessach,[1] Philipp A. Lang,[7] Pietro Luigi Poliani,[6] Silvia Giliani,[5] Waleed Al-Herz,[8] Morton J. Cowan,[9] Jennifer M. Puck,[9] Jack Bleesing,[10] Tim Niehues,[11] Catharina Schuetz,[12] Harry Malech,[13] Suk See DeRavin,[13] Fabio Facchetti,[6] Andrew R. Gennery,[14] Emma Andersson,[1] Naynesh R. Kamani,[15] JoAnn Sekiguchi,[16] Hamid M. Alenezi,[8] Javier Chinen,[17] Ghassan Dbaibo,[18] Gehad ElGhazali,[19] Adriano Fontana,[4] Srdjan Pasic,[20] Cynthia Detre,[2] Cox Terhorst,[2] Frederick W. Alt,[3] and Luigi D. Notarangelo[1]

[1]Division of Immunology and The Manton Center for Orphan Disease Research, Children's Hospital, [2]Division of Immunology, Beth Israel Deaconess Medical Center, and [3]Immune Disease Institute, Harvard Medical School, Boston, MA 02115
[4]Division of Clinical Immunology, University Hospital Zürich, CH-8091 Zurich, Switzerland
[5]Nocivelli Institute for Molecular Medicine, Pediatric Clinic, and [6]Department of Pathology, University of Brescia, 25123 Brescia, Italy
[7]The Campbell Institute for Breast Cancer Research, Ontario Cancer Institute, Department of Immunology, University of Toronto, Toronto, M5G 2M9 Ontario, Canada
[8]Allergy and Clinical Immunology Unit, Pediatric Department, Al-Sabah Hospital, 70459 Kuwait City, Kuwait
[9]Department of Pediatrics, University of California, San Francisco (UCSF) School of Medicine and UCSF Children's Hospital, San Francisco, CA 94143
[10]Children's Hospital Medical Center, Cincinnati, OH 45229
[11]Centre for Child Health and Adolescence, Helios Klinikum Krefeld Academic Hospital, Heinrich Heine University of Düsseldorf, D-02151 Düsseldorf, Germany
[12]Department of Pediatrics and Adolescent Medicine, University Hospital Ulm, D-89070 Ulm, Germany
[13]Laboratory of Host Defenses, National Institute of Allergy and Infectious Diseases, Bethesda, MD 20892
[14]Institute of Cellular Medicine, University of Newcastle, Newcastle upon Tyne, NE2 4HH England, UK
[15]Center for Cancer and Blood Disorders, Children's National Medical Center, Washington DC 20010
[16]Department of Internal Medicine, University of Michigan, Ann Arbor, MI 48109
[17]Section of Allergy and Immunology, Department of Pediatrics, Texas Children's Hospital, Baylor College of Medicine, Houston, TX 77030
[18]Department of Pediatrics and Adolescent Medicine, American University of Beirut, 1107 2020 Beirut, Lebanon
[19]Department of Immunology, Faculty of Medicine, King Fahad Medical City, 11525 Riyadh, Saudi Arabia
[20]Department of Pediatric Immunology, Mother and Child Health Institute, 11070 Beograd, Serbia

The contribution of B cells to the pathology of Omenn syndrome and leaky severe combined immunodeficiency (SCID) has not been previously investigated. We have studied a *mut/mut* mouse model of leaky SCID with a homozygous *Rag1* S723C mutation that impairs, but does not abrogate, V(D)J recombination activity. In spite of a severe block at the pro–B cell stage and profound B cell lymphopenia, significant serum levels of immunoglobulin (Ig) G, IgM, IgA, and IgE and a high proportion of Ig-secreting cells were detected in *mut/mut* mice. Antibody responses to trinitrophenyl (TNP)–Ficoll and production of high-affinity antibodies to TNP–keyhole limpet hemocyanin were severely impaired, even after adoptive transfer of wild-type CD4+ T cells. *Mut/mut* mice produced high amounts of low-affinity self-reactive antibodies and showed significant lymphocytic infiltrates in peripheral tissues. Autoantibody production was associated with impaired receptor editing and increased serum B cell–activating factor (BAFF) concentrations. Autoantibodies and elevated BAFF levels were also identified in patients with Omenn syndrome and leaky SCID as a result of hypomorphic *RAG* mutations. These data indicate that the stochastic generation of an autoreactive B cell repertoire, which is associated with defects in central and peripheral checkpoints of B cell tolerance, is an important, previously unrecognized, aspect of immunodeficiencies associated with hypomorphic *RAG* mutations.

CORRESPONDENCE
Luigi D. Notarangelo M.D:
luigi.notarangelo@childrens.harvard.edu
OR
Frederick W. Alt:
alt@enders.tch.harvard.edu

Abbreviations used: ANA, antinuclear antibody; AP, alkaline phosphatase; BAFF, B cell–activating factor; BAFF-R, BAFF receptor; HRP, horseradish peroxidase; ISC, Ig-secreting cell; MZ, marginal zone; nT reg cell, natural regulatory T cell; PB, plasmablast; PC, plasma cell; pPB, pre-PB; ssDNA, single-stranded DNA; TD, T dependent; TI, T independent; TLR, toll-like receptor.

The Rockefeller University Press $30.00
J. Exp. Med. Vol. 207 No. 7 1541-1554
www.jem.org/cgi/doi/10.1084/jem.20091927

The Journal of Experimental Medicine

B cells are generated in the bone marrow, where stochastic rearrangements of the variable (V), diversity (D), and joining (J) elements within the Ig heavy and light chains lead to development of the primary B cell repertoire (Alt and Baltimore, 1982). This process, known as V(D)J recombination, strictly requires expression of the lymphoid-specific *RAG1* and *RAG2* genes (Schatz et al., 1989; Oettinger et al., 1990). A large proportion of immature B cells that are produced in the bone marrow express a BCR that recognizes self antigens (Wardemann et al., 2003). Security checkpoints in the bone marrow and in the periphery allow purging of self-reactive B cells. In particular, BCR cross-linking by self-antigens arrests B cell development and promotes persistent expression of *RAG* gene and Ig light chain gene rearrangement (Gay et al., 1993; Tiegs et al., 1993; Radic et al., 1993). As a result of this process, also known as receptor editing, self-reactive receptors are replaced by a non–self-reactive repertoire. In addition, immature B cells that bind self-antigens with high affinity are rapidly deleted in the bone marrow (Halverson et al., 2004). Persistent and low-affinity interaction of B cells with self antigens induces a state of unresponsiveness. These anergic self-reactive B cells can be exported to the periphery, where a secondary checkpoint of B cell tolerance takes place (Melchers, 2006; Merrell et al., 2006; Miller et al., 2006). Differentiation of transitional to mature Fo (follicular) or marginal zone (MZ) B cells and development of B-1 cells are dictated by the strength of BCR signaling and by response to other survival factors that shape the preimmune B cell repertoire (Khan et al., 1995; Hayakawa et al., 1999; Cariappa et al., 2001; Pillai et al., 2004; Stadanlick and Cancro, 2008). Among survival factors that may modulate peripheral B cell fate, a key role is played by B cell–activating factor (BAFF). Anergic self-reactive B cells express lower amounts of BAFF receptor (BAFF-R) and, hence, are at a disadvantage to non–self-reactive B cells in their response to BAFF (Lesley et al., 2004). Therefore, at physiological concentrations BAFF contributes to purging of self-reactive B cells in the periphery.

RAG mutations in humans are associated with heterogeneous clinical phenotypes. Although complete lack of RAG activity leads to an SCID phenotype with absence of mature T and B cells (T^- B^- SCID; Schwarz et al., 1996), hypomorphic *RAG* mutations allow limited generation and export of T cells, and sometimes B cells, to the periphery (Villa et al., 2001). This leaky SCID condition may associate with severe manifestations of immune dysregulation, as exemplified by Omenn syndrome, which is characterized by erythroderma, lymphadenopathy, and inflammatory gut disease associated with tissue-infiltrating T lymphocytes (Villa et al., 1998). A novel and milder phenotype of leaky SCID, characterized by granuloma formation, Epstein-Barr Virus-related lymphoma and survival into late childhood, has been recently described (Schuetz et al., 2008). In the past, investigation of the immunopathology of Omenn syndrome and leaky SCID has been hampered by the lack of adequate animal models. Three mouse models carrying hypomorphic *Rag* mutations have been described that mimic Omenn syndrome or leaky SCID (Marrella et al., 2007; Khiong et al., 2007; Giblin et al., 2009). Investigation of the molecular and cellular basis of immune dysregulation in these models and in patients has been largely restricted to the analysis of T cell development, function, and tolerance (Cavadini et al., 2005; Marrella et al., 2007; Khiong et al., 2007; Giblin et al., 2009; Poliani et al., 2009). However, the possible contribution of B lymphocytes to the immunopathology of Omenn syndrome and leaky SCID has been neglected.

We hypothesized that hypomorphic *RAG* mutations may result in the generation of a residual number of peripheral B cells that contain self-reactive BCR specificities as a result of defects of receptor editing. We also hypothesized that the B cell lymphopenic environment secondary to hypomorphic *RAG* mutations may result in increased BAFF levels that can impact on competition for survival signals in the periphery and, thus, rescue self-reactive B cells. By studying a homozygous $Rag1^{S723C}$ (*mut/mut*) mouse model of leaky SCID, as well as patients with *RAG*-dependent Omenn syndrome and leaky SCID, we now report for the first time that defects in the mechanisms of B cell tolerance and altered distribution and maturation of peripheral B cells are integral components of the immunopathology of these disorders.

RESULTS

Mut/mut mice have a severe but incomplete block in B cell development

Flow cytometric analysis revealed a severe but incomplete developmental block at the pro–B cell stage in the bone marrow of 8-wk-old *mut/mut* mice, as indicated by the increased proportion of $B220^+$ IgM^- $CD43^+$ pro–B cells and decreased proportion of $B220^+$ IgM^- $CD43^-$ pre–B cells. Virtually no immature and mature recirculating $B220^+$ IgM^+ B cells were present (Fig. 1 A). Furthermore, both the proportion and the absolute number of splenic transitional (T) 1 to T3 cells, Fo1 and Fo2 cells, and MZ precursors and mature MZ B cells were dramatically decreased in *mut/mut* mice; however, they showed accumulation of $B220^{int}$ $CD93^{hi}$ cells (Fig. 1 B). CD93 (AA4.1) is a marker of immature B cells that is reexpressed during terminal B cell differentiation from pre-plasmablasts (PBs [pPBs]) to plasma cells (PCs; Chevrier et al., 2009). The $B220^{int}$ $CD93^{hi}$ B cell population in the spleen of *mut/mut* mice included both $CD138^-$ pPB and $CD138^+$ PC. Furthermore, the proportion of switched B cells that expressed surface IgG1 or IgG2a was also significantly increased (Fig. 1 B). To better define the maturation stage of $B220^+$ cells in the spleen of *mut/mut* mice, we stained them for BAFF-R, which is not expressed in early B cell progenitors. We found that *mut/mut* splenic $B220^+$ cells expressed BAFF-R at levels comparable to $B220^+$ cells from wild-type mice (unpublished data), confirming that most splenic $B220^+$ cells were mature B lymphocytes. Immunoscope profiling of negatively selected B cell–enriched splenocytes demonstrated a highly restricted pattern of the peripheral B cell repertoire in *mut/mut* mice as compared with wild-type controls (Fig. S1). Immunofluorescence staining of the spleen from *mut/mut* mice revealed absence of follicles and germinal centers but accumulation of PC in the extrafollicular areas (Fig. S2).

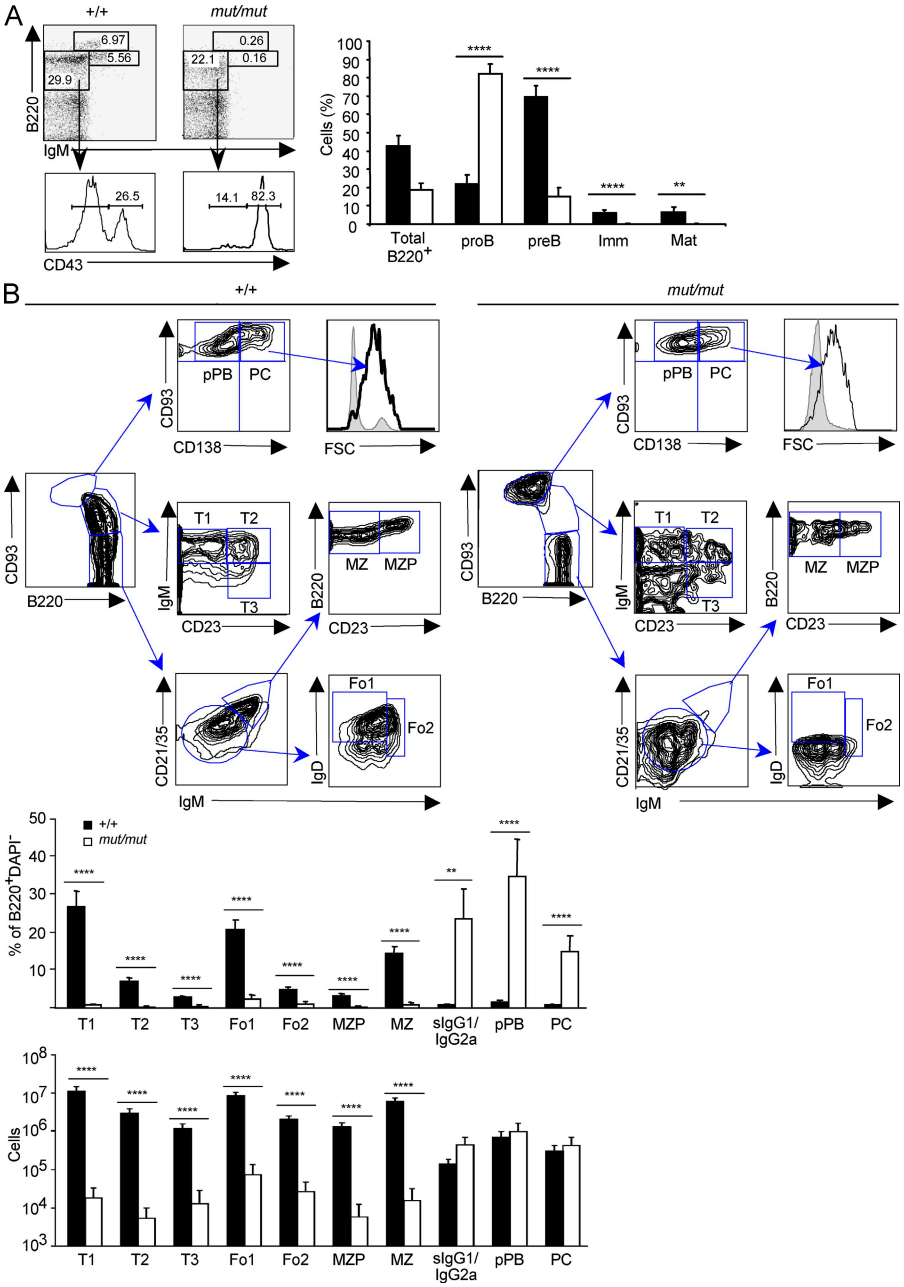

Figure 1. *Rag1*^{S723C} *mut/mut* mice have a severe but incomplete block in B cell development. (A) Distribution of B lymphocyte subsets in the bone marrow. Left: representative FACS analysis of bone marrow cells from indicated 8-wk-old mice labeled with B220 and IgM antibodies, and histograms of CD43 expression gated on B220^{+} IgM^{-} subset. Right: Percentage (mean and SD) of indicated bone marrow B cell subsets in *Rag1*^{S723C} (*mut/mut*) and wild type (+/+) mice. Imm, immature B cells; Mat, mature recirculating B cells. P-values (**, $P < 0.01$; ****, $P < 0.001$) were determined by the Mann-Whitney *U* test. Seven mice per group were analyzed in three experiments. (B) Distribution of B lymphocyte subsets in the spleen. Top: strategy for gating on transitional (T1-3), MZ precursor (MZP), Fo type I and II (Fo1-2), MZ B cells, CD93^{hi} B220^{int} CD138^{-} pPB, and CD93^{hi} B220^{int} CD138^{+} PC subpopulations of splenic B cells after excluding DAPI^{+}, Dump^{+}(CD11c, CD11b, and Gr-1), and B220^{-} cells. One representative example is shown for both wild-type (+/+) and *mut/mut* mice out of three wild-type (+/+) and seven *mut/mut* 8-wk-old mice that were analyzed in two experiments. Bottom: distribution (percentage of B220^{+} splenocytes) and absolute numbers (mean ± SD) of splenic B cell subsets, defined as in A, in 8-wk-old wild-type (+/+, $n = 3$) and *mut/mut* ($n = 7$) mice. sIgG1/sIgG2a, lymphocytes expressing surface IgG1 or surface IgG2a. P-values (**, $P < 0.01$; ****, $P < 0.001$) were determined by the Mann-Whitney *U* test.

Consistent with the relative expansion of terminally differentiated B cells, Ig serum levels were largely preserved in *mut/mut* mice (Fig. 2 A). In particular, serum levels of IgG1, IgG2a, and IgE were higher in 8-wk-old *mut/mut* mice than in age-matched controls. IgA serum levels were initially low but normalized by 16 wk of age (unpublished data). In keeping with the restricted diversity of peripheral B cell repertoire, an oligoclonal profile of Igs was demonstrated by serum electrophoresis and immunofixation in 8-wk-old *mut/mut* mice (Fig. S3 A).

To confirm that the splenic B cell compartment of *mut/mut* mice is skewed to Ig-secreting cells (ISCs), we performed ELISPOT assays in 12-wk-old mice and found a higher proportion of IgM-, IgG1-, IgG2a-, and IgA-secreting cells in the spleen of *mut/mut* mice than in wild-type mice (IgM ISC, $P < 0.05$; IgG1, $P < 0.05$; IgA, $P < 0.005$; Fig. 2 B). Molecular markers can be used to track maturation of B cells in the periphery. In particular, Ig heavy chain class switch recombination is marked by expression of post-switch transcripts, whereas differentiation from B220^{int} CD93^{hi} CD138^{-} pPB to B220^{int} CD93^{hi} CD138^{+} ISCs is accompanied by progressive decrease of *Pax5* and *Blc6* expression and up-regulation of the Blimp-1, Xbp-1, and Irf-4 transcription factors (Muramatsu et al., 2000; Reimold et al., 2001; Chevrier et al., 2009). In keeping with a high proportion of B220^{int} CD93^{hi} cells, many of which co-express CD138 and have a large size, we found that splenic B cells from naive *mut/mut* mice express high levels of Xbp-1 and of Iμ-Cγ1 switch transcripts (Fig. 2 C).

Antibody responses and dysregulation of B cell–mediated immunity in *mut/mut* mice

Next, we analyzed the ability of *mut/mut* mice to mount antibody responses to T-independent (TI) and T-dependent (TD)

antigens. At day 14 after immunization with the TI antigen TNP-Ficoll, production of both IgM and IgG3 anti-TNP antibodies was reduced in *mut/mut* mice as compared with wild-type controls ($P < 0.0001$ and $P < 0.005$ for IgM and IgG3 TNP-specific responses, respectively; Fig. 3, A and B). However, higher levels of TNP-binding IgM antibodies were detected in nonimmunized *mut/mut* mice ($P < 0.05$; Fig. 3 A). Naive *mut/mut* mice also had higher levels of low-affinity TNP-reactive IgG antibodies than wild-type mice ($P < 0.0001$; Fig. 3 C), but the TNP-specific total IgG response after primary and secondary immunization with the TD antigen TNP-KLH was blunted (Fig. 3 C). Furthermore, levels of high-affinity TNP-specific IgG antibodies after primary immunization with TNP-KLH were significantly lower in *mut/mut* mice versus controls ($P < 0.0001$; Fig. 3 D), and only a modest increase was observed after secondary immunization, as compared with a 30-fold increase in wild-type mice (Fig. 3 D, *mut/mut* vs. wild-type mice; $P < 0.0001$). These data indicate a severe defect of affinity maturation in *mut/mut* mice.

It has been previously shown that *mut/mut* mice have an abnormal T cell compartment, with reduced number of peripheral T cells, most of which express activation markers (Giblin et al., 2009). To evaluate whether lack of robust and high-affinity responses to TD antigens in *mut/mut* mice might simply reflect lack of adequate helper T cell activity, we performed adoptive transfer experiments. *Mut/mut* mice were injected i.v. with 3×10^6 purified splenic $CD4^+$ T cells from either wild-type or *mut/mut* mice, before immunization with TNP-KLH. To control whether the amount of adoptively transferred wild-type $CD4^+$ T cells was sufficient to support specific antibody production and affinity maturation, the same amount of $CD4^+$ T cells were transfused into $Zap70^{-/-}$ mice, which lack peripheral T cells but have an intact and diversified repertoire of B lymphocytes (Negishi et al., 1995). As shown in Fig. 3 (E and F), adoptive transfer of wild-type $CD4^+$ splenic T cells allowed production of a robust high-affinity TNP-specific antibody response in $Zap70^{-/-}$ mice, but not in *mut/mut* mice, upon immunization with TNP-KLH. Altogether, these data indicate that naive *mut/mut* mice spontaneously produce higher amounts of low-affinity antibodies but fail to mount robust antibody responses upon challenge with either TI or TD antigens, and that the severe impairment of high-affinity antibody response to TD antigens is not simply a result of lack of adequate helper T cell activity.

Because elevated levels of Igs (and especially IgG2a) and spontaneous production of low-affinity antibodies are often associated with the presence of self-reactive specificities (Kang et al., 1988), we screened *mut/mut* mice for the presence of autoantibodies. Titers of anti–single-stranded DNA (ssDNA) and anti-chromatin (DNA/histone) antibodies were significantly increased in 8- and 16-wk-old *mut/mut* mice, compared with age-matched wild-type mice, but normalized by 6–8 mo

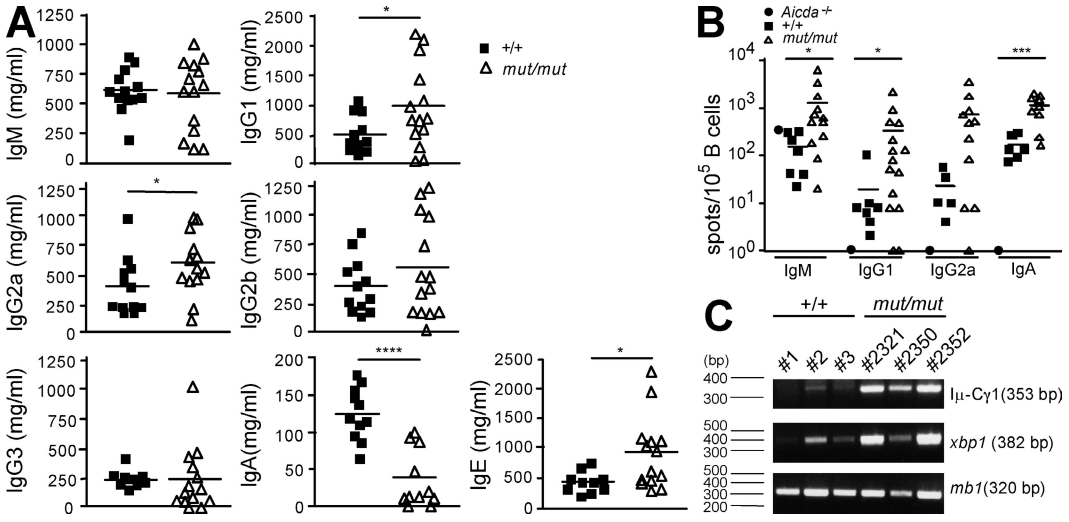

Figure 2. Ig serum levels and analysis of splenic ISCs in *mut/mut* mice. (A) Sera from 8-wk-old naive wild-type ($n = 11–13$) and $Rag1^{S732C}$ *mut/mut* ($n = 11–14$) mice were collected and IgG1, IgG2a, IgG2b, IgG3, IgM, IgA, and IgE concentrations were determined by ELISA in three independent experiments, and three to five mice for each strain (+/+ or *mut/mut*) were included in each experiment. Horizontal bars identify mean values. P-values (*, $P < 0.05$; ****, $P < 0.001$) were determined by a Student's *t* test for unpaired data. (B) The proportion of ISCs among the B cell–enriched fraction of splenocytes of 12-wk-old wild-type and *Rag1 mut/mut* mice was analyzed by ELISPOT assay for IgM (+/+ $n = 7$; *mut/mut* $n = 12$), IgG1 (+/+ $n = 7$; *mut/mut* $n = 15$), IgG2a (+/+ $n = 5$; *mut/mut* $n = 11$), and IgA (+/+ $n = 6$; *mut/mut* $n = 10$). Splenocytes were enriched for B cells by negative selection. Spots were counted by an ELISPOT Reader using a size range of 0.005–1 mm. Results are expressed as mean ± SD. Horizontal bars identify mean values. P-values (*, $P < 0.05$; ***, $P < 0.005$) were determined by the Mann-Whitney *U* test. Three ELISPOT experiments were performed that included both +/+ and *mut/mut* B cell–enriched splenocytes. The enriched splenic B cell preparation from one $Aicda^{-/-}$ mouse was tested in parallel in each experiment to confirm specificity of detection of switched isotypes. (C) RT-PCR amplification of Iμ-Cγ1 post-switch transcripts and of *xbp1* transcripts from cDNA prepared from B cell–enriched (CD90 negative) splenocytes from wild-type (+/+, $n = 3$) and *mut/mut* ($n = 3$) mice. Expression of *mb1* transcript was analyzed as internal control. One representative example of three replicates of the RT-PCR reaction is shown. The molecular size of amplified cDNAs is indicated in parentheses.

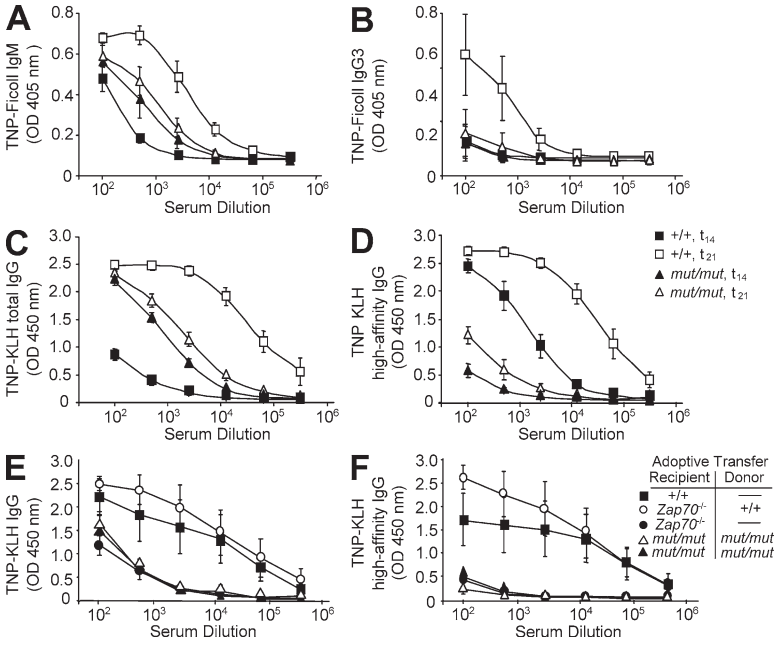

Figure 3. *Mut/mut* mice spontaneously produce low-affinity antibodies but fail to respond to immunization with TI and TD antigens. Serum levels of IgM (A) and IgG3 (B) anti-TNP antibodies were measured before (t_0) and 14 d after (t_{14}) immunization with the TI antigen TNP-Ficoll in 8-wk-old wild-type (+/+, $n = 4$) and *mut/mut* mice ($n = 5$) mice. (C) Levels of total TNP-reactive serum IgG antibodies were analyzed before (t_0) and 7 d after (t_{21}) secondary immunization with the T cell–dependent antigen TNP-KLH in wild-type (+/+, $n = 5$) and *mut/mut* ($n = 5$) mice. (D) Serum levels of high-affinity TNP-specific IgG antibodies were analyzed 2 wk after primary immunization (t_{14}) and 1 wk after secondary immunization (t_{21}) in wild-type (+/+, $n = 5$) and *mut/mut* ($n = 5$) mice. (E) Levels of total TNP-reactive serum IgG antibodies 7 d after secondary immunization in +/+, *mut/mut*, and *Zap70*$^{-/-}$ mice, with or without adoptive transfer of purified splenic CD4$^+$ T cells from *mut/mut* or +/+ mice, as indicated. Five mice per group were analyzed. (F) Serum levels of high-affinity TNP-specific IgG antibodies were analyzed 1 wk after secondary immunization in +/+, *mut/mut*, and *Zap70*$^{-/-}$ mice with or without adoptive transfer of purified splenic CD4$^+$ T cells from *mut/mut* or +/+ mice, as indicated. Five mice per group were analyzed. In all panels, results are expressed as mean ± SD values of OD. For each dilution of serum, three replicates were run in parallel. For the experiments shown in A–D, two separate sets of immunizations were performed for both TNP-Ficoll and TNP-KLH immunization of +/+ and *mut/mut* mice, and each set included two to three mice per genotype. Sera were collected at the indicated time points and levels of specific antibodies were measured in three independent ELISA experiments, each of which included all sera.

of age (Fig. 4, A and B). When sera from three mice with high concentrations of anti-ssDNA IgG were tested for the presence of κ and λ light chains, reactivity against ssDNA was detected only for κ-, but not λ-containing Igs (Fig. S4 A). Furthermore, using an immunofluorescence assay on Hep2 target cells, we found that 16/29 (55.2%) sera of 8–16-wk-old *mut/mut* mice contained autoantibodies with different specificities (Fig. S4 B), versus only 2/16 (12.5%) autoantibody-positive sera from age-matched wild-type controls (Fig. 4 C). The presence of broadly reactive autoantibodies in *mut/mut* mice was also confirmed by immunohistochemistry using a variety of tissues (skin, stomach, large bowel, kidney, salivary glands, and muscles) from *rag2*$^{-/-}$ mice as targets (Fig. S5 A and not depicted). We took advantage of the cohort of *mut/mut* mice that had received adoptive transfer of wild-type CD4$^+$ T cells to assess whether this could modulate autoantibody production. However, no significant changes were recorded in the levels of anti-chromatin IgG for up to 54 d after adoptive transfer (Fig. S6).

IgM and C3 deposits were demonstrated by immunofluorescence in kidney sections from 8-mo-old *mut/mut* mice (Fig. S5 B) but were not associated with proteinuria. Furthermore, no proteinuria was found in a cohort of 16 *mut/mut* mice from 3 to 8 mo of age. Autoantibodies may have a different pathogenicity profile depending on their affinity for self antigens. To assess the affinity of anti-ssDNA antibodies in *mut/mut* mice, we analyzed antigen binding at various salt concentrations and compared the profile to that observed in the serum of NZM2410 mice, a model of systemic lupus erythematosus with high-affinity autoantibodies. As shown in Fig. 4 D, anti-ssDNA antibodies in *mut/mut* mice were of low affinity.

Immunohistochemical analysis showed that the majority of *mut/mut* mice had prominent inflammatory infiltrates, which included T and B lymphocytes, in various target organs (Fig. S7 and Table S1). However, this immunopathology was not associated with reduced survival or weight loss in the vast majority of *mut/mut mice*, and only 4% of them developed features of Omenn syndrome (hair loss and severe colitis). Altogether, these data indicate that homozygosity for a hypomorphic *Rag1* mutation in *mut/mut* mice is associated with production of broadly reactive low-affinity autoantibodies and inflammatory infiltrates, with potential for significant immunopathology in vivo.

Defective checkpoints of B cell tolerance in *rag1 mut/mut* mice

Receptor editing is the primary mechanism by which autoreactive B cells change their BCR specificity in the bone marrow. Reexpression of the *RAG* genes is strictly necessary for receptor editing to occur. We hypothesized that hypomorphic *Rag1* mutation in *mut/mut* mice may impair receptor editing, thus facilitating persistence of self-reactive B cells. The efficiency of receptor editing can be evaluated by measuring Vκ-RS rearrangement (Panigrahi et al., 2008), in which an upstream Vκ gene element is joined to a noncoding RS element located 25 kb downstream of the Cκ element (Durdik et al., 1984; Daitch et al., 1992). The highest levels of RS rearrangement are found in bone marrow small pre–B II cells (Panigrahi et al., 2008), corresponding to Hardy's classification Fraction D bone marrow cells, which also express *Rag1* and *Rag2* genes (Hardy et al., 1991). To further highlight the importance of RS rearrangement in receptor editing and

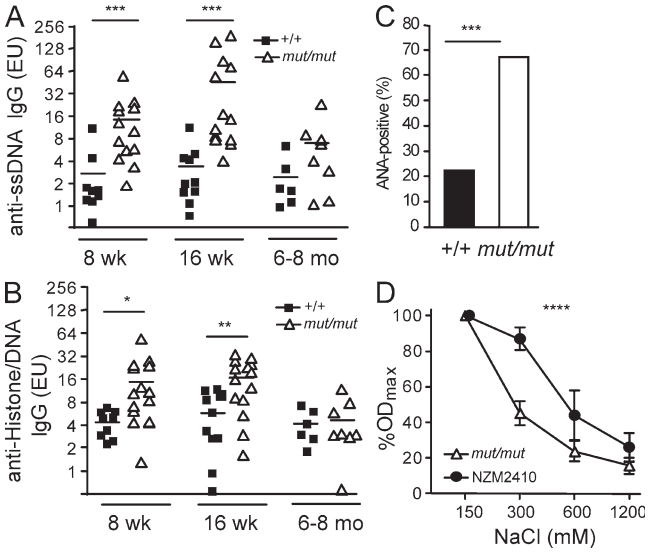

Figure 4. Autoantibodies in *mut/mut* mice. (A) Serum levels of IgG autoantibodies to ssDNA in wild-type (+/+) and *mut/mut* mice at 8 wk (+/+, $n = 9$; *mut/mut*, $n = 13$), 16 wk (+/+, $n = 10$; *mut/mut*, $n = 13$), and 6–8 mo (+/+, $n = 6$; *mut/mut*, $n = 8$) of age. P-values (***, $P < 0.005$) were determined by the Mann-Whitney *U* test. (B) IgG autoantibodies to chromatin (histone–DNA complex) in +/+ and *mut/mut* mice at 8 wk (+/+, $n = 9$; *mut/mut*, $n = 14$), 16 wk (+/+, $n = 10$; *mut/mut*, $n = 14$), and 6–8 mo (+/+, $n = 6$; *mut/mut*, $n = 8$) of age. In A and B, horizontal bars represent mean values. Results are expressed as ELISA units (EU), derived from serial dilutions of ANA-positive NZM2410 serum pool. For each serum sample, two replicates were run in parallel, and three experiments were performed. P-values (*, $P < 0.05$; **, $P < 0.01$) were determined by the Mann-Whitney *U* test. (C) Proportion of 8–16-wk-old wild-type (+/+, $n = 16$) and *mut/mut* mice ($n = 29$) whose serum contained ANAs, as measured using Hep2 immunofluorescence staining. The number of mice analyzed in each group is indicated on top of the bars. P-values (***, $P = 0.005$) were determined by the χ^2 test. (D) Affinity of anti-ssDNA IgG antibodies was measured by ELISA, using increasing salt concentrations, in the serum of *mut/mut* ($n = 8$) and NZM2410 ($n = 7$) mice. For this experiment, sera of *mut/mut* mice with high levels of anti-ssDNA IgG were used. For each serum sample, two replicates were run in parallel, and three experiments were performed. Results are expressed as mean percentage (±SD) of the OD observed at physiological (150 mM) NaCl concentration. P-values (****, $P = 0.001$) were determined by two-way ANOVA.

purging of self-reactive B cells, deletion of the RS element in mice has been found to cause persistence of autoreactive B cells in the periphery (Vela et al., 2008). We analyzed the levels of RS rearrangement in $B220^+$ $CD43^-$ $AA4.1^+$ IgM^- sorted Fraction D bone marrow B cells from *mut/mut* and control mice. A striking defect of RS rearrangement was observed in *mut/mut* mice (Fig. 5 A), thus establishing that the *Rag1* S723C mutation strongly impairs receptor editing. It has been shown that impairment of receptor editing in mice is associated with a decreased proportion of B lymphocytes expressing λ light chains (Vela et al., 2008). This was also the case in *mut/mut* mice, in which λ^+ cells were only 0.43 ± 0.61 (mean ± SD) % of $B220^{hi}$ splenic B cells, as compared with 2.46 ± 0.42% in wild-type controls ($P < 0.001$, $n = 5$ for both groups).

Under normal circumstances, self-reactive B cells that escape deletion or receptor editing in the bone marrow are purged at a peripheral checkpoint, where they compete with non–self-reactive B cells for survival signals. BAFF is a key factor that may modulate survival of peripheral B cells beyond the T1 stage of differentiation, when BAFF-R begins to be expressed (Hsu et al., 2002; Darce et al., 2007a,b). There is evidence both in mice and in humans that BAFF levels are regulated by the number of peripheral B cells, with higher levels being detected in B cell lymphopenic hosts (Cambridge et al., 2006; Lavie et al., 2007). Consistent with this, serum BAFF levels were markedly higher in *mut/mut* mice than in control mice both at 8 and 16 wk of age (Fig. 5 B). However, lower BAFF serum levels were detected in *mut/mut* mice at 9–10 mo of age as compared with 8- or 16-wk-old *mut/mut* mice (Fig. 5 B) This decrease was inversely correlated with an increase in the absolute number of $B220^+$ splenic B cells in 9–10-mo-old versus 16-wk-old *mut/mut* mice (mean ± SD, 13.0 ± 3.8 vs. $3.8 \pm 1.9 \times 10^6$ cells, $P = 0.0013$; $n = 5$ for both groups) and was associated with normalization of the levels of anti-ssDNA and anti-chromatin antibodies (Fig. 4, A and B).

Increased BAFF levels and autoantibodies in patients with *RAG*-dependent immunodeficiency

The results obtained in *mut/mut* mice prompted us to analyze sera of patients with *RAG*-dependent immunodeficiencies for evidence of B cell–mediated autoimmunity. In spite of a severe B cell lymphopenia, patients with leaky SCID and with Omenn syndrome as a result of hypomorphic *RAG* mutations often have residual Ig serum levels, and IgEs in particular are typically increased (Villa et al., 2001; Sobacchi et al., 2006), arguing for the presence of ISCs. However, humoral immunity in these patients has received little attention in the literature. We have analyzed BAFF serum levels and autoantibodies in a cohort of patients with various forms of combined immunodeficiency and in 11 age-matched healthy infants. As shown in Fig. 6, serum BAFF levels were 10-fold higher in patients with *RAG* and Artemis deficiency than in controls and were also higher than in patients with X-linked SCID (SCIDX1), a condition characterized by lack of circulating T and NK lymphocytes but a normal number of B cells.

As shown in Table I, serum autoantibodies were detected in the majority (9 out of 14) of patients with hypomorphic *RAG* mutations leading to Omenn syndrome or leaky SCID. In contrast, none of the 14 patients with SCIDX1 had detectable autoantibodies (Omenn/leaky SCID vs. SCIDX1, $P < 0.0005$), and only 1 out of 6 control infants tested borderline positive (1:40) for antinuclear antibodies (ANAs). Among patients with hypomorphic *RAG* mutations, ANA (at a titer of 1:80 or greater) were more commonly detected and were shown to be of IgM isotype. We tested sera from four patients with Omenn syndrome caused by hypomorphic *RAG* mutations for oligoclonality by electrophoresis and immunofixation, and one such serum showed a restricted pattern (Fig. S3 B). These results demonstrate that increased autoantibody production and

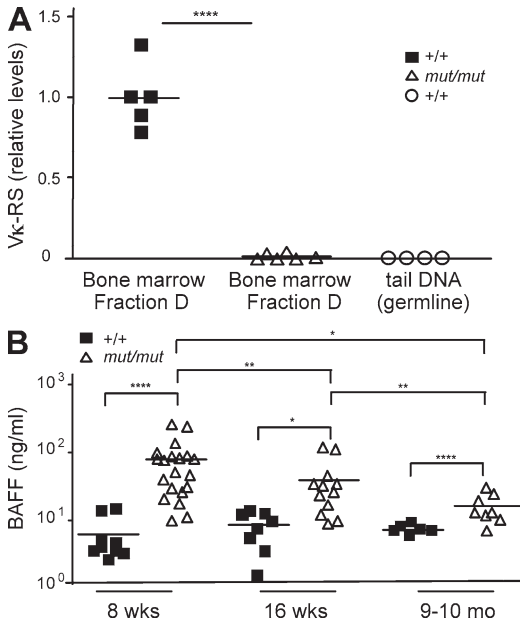

Figure 5. Impaired receptor editing and increased serum BAFF levels in *mut/mut* mice. (A) Levels of Vκ-RS DNA rearrangement products were measured by quantitative PCR in sorted bone marrow $B220^+$ $CD43^-$ $AA4.1^+$ IgM^- (Fraction D) cells from wild-type (+/+, *n* = 4) and *mut/mut* (*n* = 5) mice. Results were expressed as relative levels of Vκ-RS DNA rearrangement products as compared with a reference value of 1 attributed to DNA from sorted Fraction D bone marrow cells from one selected wild-type (+/+) mouse. Genomic DNA extracted from the tail of wild-type mice was run in parallel. For each of two experiments performed, quantitative PCR was run in triplicates. Horizontal bars identify mean values. P-values (****, $P < 0.001$) were determined by a two-tailed Student's *t* test for unpaired data. (B) Serum BAFF levels in 8-wk-old, 16-wk-old, and 9–10-mo-old wild-type (+/+, *n* = 6–8) and *mut/mut* (*n* = 8–20) mice. Horizontal bars represent mean values. For each serum sample, three replicates were run and three experiments were performed. P-values (*, $P < 0.05$; **, $P < 0.01$; ****, $P < 0.001$) were determined by a two-tailed Student's *t* test for unpaired data.

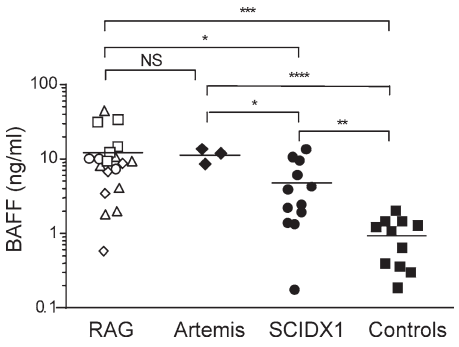

Figure 6. Serum BAFF levels in patients with *RAG* mutations. Serum BAFF levels in 19 patients with *RAG* mutations, 3 patients with T^- B^- SCID as a result of *DCLRE1C* (Artemis) deficiency, 12 patients with X-linked SCID (SCIDX1), and 11 age-matched controls. Different symbols identify distinct clinical phenotypes associated with *RAG* mutations as follows: □, T^- B^- SCID; △, Omenn syndrome; ○, leaky SCID; ◇, leaky SCID with granuloma. Horizontal bars represent mean value. For each serum sample, three replicates were run and three experiments were performed. P-values (*, $P < 0.05$; **, $P < 0.01$; ***, $P < 0.005$; ****, $P < 0.001$) were determined by a two-tailed Student's *t* test for unpaired data.

elevated BAFF serum levels are frequently also observed among patients with hypomorphic *RAG* defects.

DISCUSSION

Immune dysregulation is increasingly being recognized as a prominent feature of genetically determined immunodeficiencies (Carneiro-Sampaio and Coutinho, 2007; Liston et al., 2008; Pessach et al., 2009). *RAG* mutations in humans may cause complete or partial defects of V(D)J recombination and, hence, result in SCID or in a leaky phenotype with residual T (and sometimes B) cell development associated with immune dysregulation and skewing of the T lymphocyte repertoire (Signorini et al., 1999). We and others have previously shown that the reduced thymopoiesis in patients with Omenn syndrome and leaky SCID is accompanied by defects in thymic epithelial cell maturation and/or homeostasis, impaired expression of aire (autoimmune regulator) protein and poor generation and function of $CD4^+$ $CD25^+$ $Foxp3^+$ natural regulatory T cells (nT reg cells; Cavadini et al., 2005; Poliani et al., 2009; Cassani et al., 2010b). However, the possible contribution of defects in B cell tolerance to the immunopathology of Omenn syndrome and leaky SCID has not been previously investigated. *RAG*-dependent immunodeficiency is characterized by profound B cell lymphopenia (Villa et al., 2001), although residual production of antibodies (IgE in particular) and ability to mount low-affinity antibody responses to bacteriophage ϕx174 neoantigen have been reported in patients with hypomorphic *RAG* mutations (Ochs et al., 1974). Importantly, autoimmune cytopenias have been observed in several patients with Omenn syndrome or with leaky SCID caused by hypomorphic *RAG* defects (Ehl et al., 2005; de Villartay et al., 2005), implying that B cell–mediated mechanisms may contribute to the immunopathology of these diseases, The recent availability of suitable animal models has made it possible to study in greater detail B cell development, maturation, and function in conditions associated with hypomorphic *Rag* mutations. The Rag1 S723C mutant protein is proficient for DNA cleavage but exhibits severe defects in

Table I. Autoantibodies in patients with hypomorphic *RAG* mutations

Patients	*n*	*n* (%) with autoantibodies	Specificity
***RAG* deficiency**			
OS/LS	14	9 (64.3)	Five ANA, four TPO, two pANCA, one TG, and one OmpC
T^- B^- SCID	5	0 (0)	
SCIDX1	14	0 (0)	
Controls	6	1 (16.7)	ANA

OS, Omenn syndrome; LS, leaky SCID; TPO, thyroid peroxidase; pANCA, perinuclear anti-neutrophil cytoplasmic antibody; TG, thyroglobulin; and OmpC, outer membrane porin protein C.

post-cleavage complex formation and end-joining (Tsai et al., 2002; Giblin et al., 2009). Homozygosity for this mutation in *mut/mut* mice leads to a severe, although incomplete, block in B cell development but normal or even increased Ig levels. Similar observations had been previously reported in another model of leaky SCID, the MM mouse, with a homozygous *Rag1* R972Q mutation (Khiong et al., 2007). Using ELISPOT assays, detailed flow cytometric analysis, and molecular assays to track terminal B cell maturation, we have now obtained substantial evidence that the spleens from *mut/mut* mice contain an increased proportion of class-switched B cells and ISCs. Consistent with this, significant amounts of Igs of various isotypes are present in the serum of *mut/mut* mice. However, both the peripheral B cell repertoire and serum Ig profile from *mut/mut mice* show a restricted pattern. This likely reflects a limited number of productive V(D)J rearrangements as a result of the hypomorphic *Rag1* mutation. The stochastic nature of the process may also account for some variability of serum Ig levels in *mut/mut* mice, as previously reported for IgE (Giblin et al., 2009). Several mechanisms may be taken into account to explain the apparent discrepancy between the B cell production bottleneck and significant Ig production in *mut/mut* mice. Adoptive bone marrow transfer experiments have shown that when limited numbers of B cells are transferred into immunodeficient mice, a large proportion of the transferred B cells undergo homeostatic proliferation and develop into PCs (Agenès and Freitas, 1999; Cabatingan et al., 2002). Furthermore, it has been demonstrated that under in vivo inflammatory conditions, immature/T1 B cells express significant levels of activation-induced cytidine deaminase and Blimp-1 (Ueda et al., 2007). In vitro activation of immature/T1 B cells by toll-like receptor (TLR) ligands induces these cells to proliferate and secrete Igs in a TI manner (He et al., 2004). Moreover, innate immune cells are over-reactive in lymphopenic environment (Cao et al., 2009), and this may lead to increased expression of cytokines (such as BAFF) that may favor B cell survival and/or differentiation (Ueda et al., 2007). It can be speculated that the profound immunodeficiency and defects in the gut-blood barrier may render *mut/mut* mice and patients with Omenn syndrome susceptible to inflammation sustained by endogenous commensal flora, as shown in other human immunodeficiencies (Brenchley et al., 2006). Interestingly, 4% of *mut/mut* mice have developed colitis and/or erythroderma, and their spleens demonstrated very high numbers of ISCs.

We have demonstrated that *mut/mut* mice are severely impaired in the antibody response to TI and TD antigens, and in particular are unable to mount high-affinity antibody responses. Adoptive transfer of wild-type $CD4^+$ T lymphocytes was unable to correct defective antibody response to TNP-KLH, indicating that B cell–intrinsic abnormalities (including restricted B cell repertoire) and/or aberrant architecture of secondary lymphoid organs (characterized by lack of follicles and of germinal centers) account for the impaired antibody response to TD antigens in *mut/mut* mice. However, they spontaneously produce high levels of low-affinity antibodies that contain self-reactive specificities. Importantly, we have demonstrated for the first time that hypomorphic *RAG* mutations are associated with a high frequency of autoantibodies also in humans. Our data indicate that several mechanisms may be involved in generating and sustaining this B cell–mediated immune dysregulation. Normally, highly polyreactive and self-reactive B cells are counterselected at the primary B cell tolerance checkpoint in the bone marrow, mostly through receptor editing. It has been estimated that both in mice and in humans, ∼20–50% of developing B cells undergo receptor editing (Retter and Nemazee, 1998; Casellas et al., 2001; Wardemann et al., 2004). This process is accompanied by a drastic decrease in the proportion of self-reactive antibodies that are detected in early immature versus immature B lymphocytes in humans (Wardemann et al., 2003). A large fraction of autoantibodies expressed by these developing early immature B cells have low affinity for multiple antigens (i.e., are polyreactive) and contain ANAs (Wardemann et al., 2003). Using a recently developed assay which is based on quantitation of RS rearrangement at the κ locus (Panigrahi et al., 2008), we have demonstrated a drastic impairment of receptor editing in the bone marrow of *mut/mut* mice. Consistent with this, we have also found that the proportion of peripheral B lymphocytes expressing λ light chain is significantly reduced in *mut/mut* mice and that anti-ssDNA antibodies expressed κ, but not λ, light chains. Interestingly, we and others have recently reported increased levels of autoantibodies also in mice with hypomorphic mutations of DNA ligase IV (Nijnik et al., 2009; Rucci et al., 2010), another protein which is critically involved in T and B cell development and receptor editing.

Our data suggest that disturbance in peripheral checkpoints of B cell tolerance may also be involved in the pathophysiology of autoimmunity associated with hypomorphic *Rag* mutations. BAFF serum levels were 10-fold higher in *rag*-mutated mice and humans than in controls. Based on previous studies, this is likely the consequence of the B cell lymphopenic environment (Lesley et al., 2004; Lavie et al., 2007). High levels of BAFF-R are expressed by $CD21^{int}$ T2 B cells, which undergo extensive BAFF-mediated homeostatic proliferation (Meyer-Bahlburg et al., 2008). Anergic self-reactive B cells in the periphery express low levels of BAFF-R, show reduced BAFF responsiveness, and are normally lost at the T2 stage or beyond (Lesley et al., 2004; Thien et al., 2004). However, self-reactive peripheral B cells can be rescued by exogenous administration or overexpression of BAFF (Mackay et al., 1999; Lesley et al., 2004; Thien et al., 2004; Hondowicz et al., 2007) and produce anti-chromatin and anti-DNA antibodies (Hondowicz et al., 2007). It has been shown that in vivo BAFF neutralization ameliorates islet-directed autoimmunity in nonobese diabetic mice by increasing competition among transitional B cells for follicular entry (Zekavat et al., 2008). We did not have access to BAFF-neutralizing antibody and, thus, could not directly test the significance of increased BAFF levels in the autoimmunity of *mut/mut* mice. In a companion paper, Cassani et al. (in this issue) report that i.v. injection of

an anti–BAFF-R monoclonal antibody into *Rag2*^{R229Q} mice led to disappearance of anti–double-stranded DNA IgG antibodies and significant amelioration of inflammatory infiltrates. In contrast, BAFF-R–deficient A/WySnJ mice develop autoantibodies and severe glomerulonephritis (Mayne et al., 2008), indicating that balance of BAFF levels may be important to maintain B cell tolerance. Consistent with this, we found that increase of mature B cell number in older *mut/mut* mice was associated with decrease of BAFF serum levels and normalization of the titer of anti-ssDNA and anti-chromatin antibodies. Altogether, these data suggest that increased BAFF serum levels play a significant role in autoimmune manifestations associated with hypomorphic *Rag* mutations.

There is supporting evidence that elevated BAFF serum levels may also associate with immune dysregulation in humans (Moisini and Davidson, 2009). Very elevated serum BAFF concentrations were detected in our series of 19 patients with *RAG* mutations, including 14 patients with Omenn syndrome or leaky SCID, 9 of which had evidence of autoantibodies. Levels of BAFF were higher in patients with *RAG* mutations than in those with SCIDX1, none of which developed signs of autoimmunity. It is possible that a certain threshold of BAFF concentration must be reached to rescue self-reactive B cells in the periphery. However, other non–mutually exclusive mechanisms may also account for the different incidence of autoimmunity between patients with hypomorphic *RAG* defects and those with SCIDX1. Impaired receptor editing is anticipated in *RAG* deficiency but not in SCIDX1. Furthermore, patients with SCIDX1 typically lack mature T lymphocytes, whereas both in humans and in mice hypomorphic *RAG* mutations are often associated with a variable number of oligoclonal and in vivo activated T cells that infiltrate target organs and may promote and/or sustain B cell–mediated autoimmunity. In the companion manuscript, Cassani et al. (2010a) show that in vivo depletion of CD4$^+$ cells in *Rag2*^{R229Q} mice results in the decrease of ISCs and normalization of serum IgE. In contrast, autoimmunity develops to the same extent in both T cell–sufficient and in T cell–deficient BAFF-transgenic mice (Groom et al., 2002), indicating that BAFF-mediated rescue of self-reactive B cells may be T cell independent. In this regard, it is noteworthy that adoptive transfer of wild-type CD4$^+$ T cells did not ameliorate autoimmunity in *mut/mut* mice. Nonetheless, it is likely that the severe defects in T cell development and function observed in *mut/mut* mice and in patients with Omenn syndrome and leaky SCID may contribute to B cell–mediated immune dysregulation. In particular, we and others have shown that hypomorphic *RAG* mutations are associated with a severe defect in the ability to support nT reg cells development and function both in mice (Marrella et al., 2007) and in humans (Poliani et al., 2009; Cassani et al., 2010b).

We have shown that *mut/mut* mice produce polyreactive low-affinity antibodies with self-reactive specificities. Usually, such antibodies are not associated with organ-specific autoimmunity and tissue damage. Consistent with this, *mut/mut* mice did not show significant signs of disease, such as weight loss, proteinuria, or reduced life span, under SPF conditions, and only a minority (4%) of them developed alopecia or colitis. In contrast, a significant proportion of *Rag2*^{R229Q} mice develop features of Omenn syndrome by 8–10 wk of age (Marrella et al., 2007). Furthermore, >10% of *Rag2*^{R229Q} mice produce high-affinity anti–double-stranded DNA antibodies and show prominent T and B cell infiltrates in the kidney (leading to proteinuria), the gut, and the skin, as reported by Cassani et al. (2010a) in the companion paper. Several mechanisms may account for the phenotypic heterogeneity both between and within these *Rag*-mutated mouse models. It is possible that the distinct *Rag* mutations carried by these models exert a different effect on the efficiency of V(D)J recombination, generation of T and B lymphocytes, and receptor editing and that the stochastic nature of the process contributes to the heterogeneity of the phenotype, even within the same model. Moreover, it is possible that differences in housing conditions and in the microbial gut flora may modulate B cell–mediated autoimmunity through TLR-mediated signaling. Consistent with this, Cassani et al. (2010a) have shown that B lymphocytes from *Rag2*^{R229Q} mice respond efficiently to TLR agonists undergoing terminal differentiation, Ig production, and class switch recombination. Finally, T lymphocytes may also play a role in precipitating the disease phenotype. In this regard, Cassani et al. (2010a) have shown that depletion of CD4$^+$ T cells in *Rag2*^{R229Q} mice leads to reduction of ISCs and normalization of serum IgE, associated with a decrease of IL-21 and IFN-γ serum levels. These factors may contribute to the significant variability of the clinical phenotype that has also been observed in patients with hypomorphic *RAG* mutations, even within the same family (Villa et al., 2001).

In conclusion, we have established that hypomorphic *RAG* mutations in mice and humans are associated with autoantibody production. We have determined that this B cell–mediated immune dysregulation reflects profound abnormalities in the mechanisms that govern central and peripheral B cell tolerance. Experiments based on adoptive transfer of T reg cells, in vivo injection of TLR agonists, and generation of *mut/mut* mice carrying additional defects in TLR signaling may permit to define the relative contribution of impaired T cell–mediated control of B cell immune dysreactivity and TLR-mediated B cell activation to the autoimmune phenomena of leaky SCID and Omenn syndrome.

MATERIALS AND METHODS

Mouse strains. 129Sv *Rag1*^{S723C} (*mut/mut*) mice were previously generated and described (Giblin et al., 2009). *Zap70*$^{-/-}$ mice (Negishi et al., 1995), backcrossed to C57BL/6 background, were a gift from A. Singer (National Cancer Institute, Bethesda, MD). 129Sv and C57BL/6 wild-type (+/+) mice were purchased from Charles River. *Aicda*$^{-/-}$ mice were previously described (Muramatsu et al., 2000) and were a gift from T. Honjo (Kyoto University, Kyoto, Japan). Mice were housed at the Karp Family Research Building under specific pathogen-free conditions. Animal studies were approved by the Animal Care and Use Committee, Children's Hospital Boston (protocol 07–10-1445).

Patients. Sera were obtained at diagnosis, before treatment, from a total of 19 patients with molecularly confirmed *RAG*-dependent immunodeficiency (14 patients with SCIDX1, 3 patients with *DCLRE1C* (Artemis) deficiency,

and 11 age-matched controls) upon informed consent by the local Institution Review Board (IRB) and in respect to the Helsinki declaration. Human studies were approved by Children's Hospital Boston IRB, protocol 04–09-113R).

Antibodies, flow cytometry, and immunohistochemistry. For flow cytometry, the following anti–mouse antibodies were used: B220-FITC, CD21-FITC, IgM-APC, CD38-PE, Fas-PE-Cy7, CD11b-biotin, Gr-1-biotin (BD), B220–Alexa Fluor 700, AAA4.1-PE, CD23-PE-Cy7, IgD–Pacific Blue, IgM-PE-Cy5, GL7-APC, CD11c-biotin (eBioscience), and IgG1/2a-FITC (BioLegend). For biotinylated antibodies, streptavidin-PerCP was used in the secondary step. Data were acquired on a FACSCalibur cytometer (BD) and LSR flow cytometer (BD) and analyzed using FlowJo (version 8.2 for Mac; Tree Star, Inc.).

For characterization of the splenic B cell compartment, 5-µm sections of the spleens from 8-wk-old *mut/mut* and +/+ mice ($n = 4$ for each) were incubated with B220–Alexa Fluor 647, IgG–Alexa Fluor 488, IgG2a-PE (Invitrogen), and peanut agglutinin–FITC (Vector Laboratories). To detect immune complexes in the kidney glomeruli, 5-µm frozen sections were prepared from the kidneys of four 12-wk-old *mut/mut*, two 12-wk-old +/+, three 8-mo-old *mut/mut*, and two 8-mo-old +/+ mice. Glomerular immune complexes were revealed using Alexa Fluor 488–labeled anti–mouse IgM and C3 (Invitrogen). Images were acquired using a Radiance 2000MP confocal imaging system (Bio-Rad Laboratories) using 20 and 40× objectives controlled by LaserSharp software (Bio-Rad laboratories).

Immunohistochemistry of peripheral organs was performed on a total of 45 *mut/mut* and 10 +/+ mice ranging from 8 wk to 11 mo of age. 4-µm-thick sections from formalin-fixed paraffin-embedded tissue samples were stained with hematoxylin and eosin and immunostained as previously described (Poliani et al., 2009). The following primary antibodies were used: rat anti-B220 (clone RA3-6B2, 1:100; Invitrogen), rabbit anti-CD3 (1:100; Dako), and rabbit anti–Iba-1 (1:500; Wako Chemicals USA, Inc.). PCs were detected directly by using either an appropriate biotinylated goat anti–mouse IgM antibody (Vector Laboratories) or ChemMate Envision Mouse-HRP kit (Dako) that binds specifically to the mouse Ig. Digital images were acquired with a camera (DP70; Olympus) using AnalySIS software (Olympus). The degree of inflammation was scored using the following criteria: 0, none/scarce; 1, low; 2, moderate; 3, high. Colitis was graded as previously described (Scheiffele and Fuss, 2002).

To detect tissue-specific antibodies in the serum of *mut/mut* mice, 5-µm cryostat tissues from various organs (skin, stomach, small and large bowel, kidney, salivary glands, muscles, pancreas, and ovaries) of *rag2*$^{-/-}$ mice were fixed in ice-cold acetone and were incubated with 1:100 and 1:400 dilutions of serum from *mut/mut* ($n = 11$) or +/+ ($n = 6$) mice. Reactions were revealed with Alexa Fluor 488–labeled F(ab′)$_2$ anti–mouse IgG secondary antibody (Invitrogen). Slides were viewed with a microscope (Laborlux D; Leitz) using 20 and 40× Plan Neofluar objectives (Carl Zeiss, Inc.). Images were acquired with a camera (DFC 300F; Leica) and processed with FireCam software (Leica).

Analysis of ISCs by ELISPOT. Multiscreen HA plates (Millipore) were coated with 5 µg/ml of anti–mouse κ and anti–mouse λ antibodies (Southern-Biotech). Splenocytes from 12-wk-old *mut/mut*, +/+, and *aicda*$^{-/-}$ mice were enriched for B cells by negative selection using EasySep (STEMCELL Technologies Inc.), according to the manufacturer's instructions. Cells were plated in twofold dilutions starting from several groups of 10^5 cells. After overnight incubation at 37°C in 5% CO_2, the plates were washed, and IgM-, IgG1-, IgG2a-, and IgA-ISCs were detected by incubating with anti–mouse isotype-specific biotinylated antibodies (SouthernBiotech), followed by incubation with streptavidin–horseradish peroxidase (HRP) and 3-amino-9-ethylcarbazole (Sigma-Aldrich) as chromogen. Spots were counted by an Elispot Reader (Cellular Technology Ltd.) using a size range of 0.005–1 mm.

Analysis of post-switch transcripts and *Xbp1* expression. Splenocytes of 8-wk-old +/+ ($n = 3$) and *mut/mut* ($n = 3$) mice were enriched for B cells by negative selection using the CD90.2 kit (Miltenyi Biotec). Iµ-Cγ1 post-switch transcript and *Xbp1* transcript were amplified using cDNA prepared from B cell–enriched (CD90 negative) splenocytes as a template. *mb-1* transcripts were used as internal control. Primers used for Iµ-Cγ1 post-switch transcript were previously described (Muramatsu et al., 2000). The following primers were used to amplify *mb-1* and *Xbp1* transcripts: mb-1 forward, 5′-GCCAGGGGGTCTAGAAGC-3′; mb-1 reverse, 5′-TCACTTGGCACCCAGTACAA-3′; Xbp1 forward, 5′-TAGAAAGAAAGCCCGGATGAGCGA-3′; and Xbp1 reverse, 5′-TGACAGGGTCCAACTTGTCCAGAA -3′.

Immunoscope profiling of BCR. The diversity of splenic B cell repertoire was analyzed in +/+ and *mut/mut* mice ($n = 4$ for both) by immunoscope analysis. In brief, cDNA was prepared from B cell–enriched splenocytes obtained by negative selection using the CD90.2 kit. The CDR3 region of Ig heavy chain variable (V) region was amplified using a V-specific forward primer and a common reverse primer in the JH region (5′-CTTACCTGAGGAGACGGTGA-3′; Carey et al., 2008). Forward primers were the following: MIGHV1, 5′-TCCAGCACAGCCTACATGCAGCTC-3′; MIGHV2, 5′-CAGGTGCAGCTGAAGGAGTCAGG-3′; MIGHV3, 5′-AGGTGCAGCTTCAGGAGTCAGG-3′; MIGHV5, 5′-CAGCTGGTGGAGTCTGGGGGA-3′; MIGHV6, 5′-AAGTGAAGCTTGAGGAGTCTGG-3′; and MIGHV7, 5′-AGGTGAAGCTGGTGGAGTCTGG-3′.

Amplification reactions were performed using 2 ng cDNA in 50 µl of reaction containing 1 U/µl Taq Gold DNA polymerase, 200 µM dNTPs, 1 µM of each primer, and 1.5 mM $MgCl_2$ in 10× amplification buffer (Applied Biosystems). After 10 min at 95°C, amplification was performed for 40 cycles as follows: 30 s at 94°C, 30 s at 60°C, 1 min 30 s at 72°C, and ended with a step of 10 min at 72°C. Each PCR product was subjected to four runoff cycles primed with the same primer used as reverse for the PCR reaction labeled with 0.2 µM FAM in the presence of 1 U/µl Taq Gold DNA polymerase, 200 µM dNTPs, and 1.5 mM $MgCl_2$ in 10× amplification buffer. Runoff cycles are as follows: 2 min at 94°C, 2 min at 60°C, and 20 min at 72°C. PCR products were then processed on an ABI3130 Genetic analyzer (Applied Biosystems). Spectratype data were analized using GeneMapper v3.7 software (Applied Biosystems).

Analysis of receptor editing by RS rearrangement. Quantitative PCR for V_K-RS rearrangement was performed as previously described (Panigrahi et al., 2008) with slight modifications, using a protocol provided by S. Koralov (Harvard University, Boston MA). In brief, bone marrow cells from 12-wk-old +/+ ($n = 4$) and *mut/mut* ($n = 5$) mice were incubated with B220-APC, AA4.1-PECy7, IgM-PE, and CD43 FITC antibodies, and Fraction D ($B220^+$ $AA4.1^+$ IgM^- $CD43^-$) cells were sorted on a FACSAria (BD). Purity of the sorted population was consistently >97%. Genomic DNA was extracted from sorted Fraction D bone marrow cells using the Gentra Puregene Tissue kit (QIAGEN). Germline DNA isolated from the tail of four +/+ mice served as a negative control. For quantitative PCR, Power SyBR Green PCR Master Mix (Applied Biosystems) was combined with 10 ng of template DNA in a 20-µl reaction mix containing 20 pMol of forward primer (5′-AGCTTCAGTGGCAGTGGRTCWGGRAC-3′) and 20 pMol of reverse primer (5′-ACATGGAAGTTTTCCTGGGAGAATATG-3′). 40 cycles of amplification were run (95°C for 10 min, 95°C for 15 s, and 60°C for 1 min) and analyzed on an AB 7500 real-time PCR system (Applied Biosystems) using standard quantitative PCR protocol. Amplification of GADPH was run in parallel as a calibrator. The amount of V_K-RS product in each mouse sample was normalized to the amount of GAPDH and compared with the normalized target value in sorted Fraction D cells from +/+ mice (comparative $C_T[\Delta\Delta C_T]$ method). Statistical analysis was performed using Student's *t* test for unpaired data.

Immunization with TNP-Ficoll and TNP-KLH. To elicit TI antibody responses, gender-matched 8-wk-old *mut/mut* and +/+ mice were injected i.p. with 50 µg TNP-Ficoll (Biosearch Technologies). Sera were collected at the time of immunization (t_0) and 14 d later (t_{14}), and anti-TNP IgM and

IgG3 antibody titers were measured by ELISA as previously described (Tsitsikov et al., 1997), using alkaline phosphatase (AP)–conjugated goat anti–mouse IgM and IgG3, followed by reaction with *p*-nitrophenylphosphate (Sigma-Aldrich). The serum samples were run with six fivefold dilutions for determination of end-titer dilution. For TD antigen responses, gender-matched 8-wk-old *mut/mut* and +/+ mice were injected i.p. with 100 μg TNP-KLH (Biosearch Technologies) and aluminum adjuvant (Thermo Fisher Scientific) at the time of the first immunization and with 25 μg TNP-KLH for secondary immunization, 2 wk apart. Sera were collected on the day of the primary immunization (t_0), at the time of the secondary immunization (t_{14}), and 1 wk later (t_{21}) and IgM, total, and high-affinity anti-TNP IgG antibody titers were measured by ELISA using high binding Costar EIA plate (Corning). To distinguish between total and high-affinity TNP-specific IgG responses, plates were coated with TNP(18)-BSA and TNP(3)-BSA, respectively. TNP-specific IgM were detected using AP-conjugated goat anti–mouse IgM, followed by reaction with p-nitrophenylphosphate (p-NP; Sigma-Aldrich) and reading of OD at 405 nm. To detect total and high-affinity TNP-specific IgG responses, HRP-conjugated sheep anti–mouse IgG (GE Healthcare) was used, and the reaction was revealed with 3,3′,5,5′ tetramethylbenzidine (TMB; BD), followed by OD reading at 450 nm. Serum samples were run with six fivefold dilutions for end-titer determination. Statistical analysis was done using two-way ANOVA.

Adoptive CD4$^+$ T cell transfer. CD4$^+$ splenic T cells from +/+ or *mut/mut* mice were enriched by negative selection using the CD4$^+$ T cell isolation kit (Miltenyi Biotec). A total of 3×10^6 CD4$^+$ +/+ or *mut/mut* T cells were adoptively transferred into *mut/mut* mice ($n = 5$ per group). In parallel, 3×10^6 CD4$^+$ T cells from syngeneic wild-type mice were adoptively transferred into *zap70*$^{-/-}$ mice ($n = 5$). Control groups included +/+ mice and *zap70*$^{-/-}$ mice ($n = 5$ per group) that did not receive CD4$^+$ T cell transfer. 1 d after the adoptive transfer, all mice were immunized i.p. with TNP-KLH as described in the previous section, followed by a boosting immunization 2 wk later. Sera were collected at the time of primary immunization (t_0), 7 d after secondary immunization (t_{21}), and 54 d after adoptive transfer.

Determination of serum Igs by ELISA. Nunc Immuno plates (Thermo Fisher Scientific) were coated with 2.5 μg/ml of unlabeled goat anti–mouse IgM, IgG1, IgG2a, IgG2b, IgG3, IgA (SouthernBiotech), and IgE (BD). Samples were incubated on plates in a dilution ranging from 1:1,000 to 1:10,000 for IgM, 1:5,000 to 1:10,000 for IgG1 and IgG2b, 1:1,000-1:2,000 for IgG2a, 1:2,000 to 1:5,000 for IgG3, and 1:50 and 1:100 for IgE. Plates were washed and bound autoantibodies were detected with corresponding AP-conjugated goat anti–mouse IgM, IgG1, IgG2a IgG2b, IgG3 (all from BD), and IgA (SouthernBiotech) antibodies. For IgE determination, a biotinylated anti-IgE (BD) primary antibody was used, followed by streptavidin-HRP. Colorimetric reaction was produced by final incubation with *p*-nitrophenylphosphate (Sigma-Aldrich) for IgM, IgG1, IgG2a, IgG2b, IgG3, and IgA and ABTS Peroxidase substrate (KPL) for IgE. OD was measured at 405 nm and 450 nm for AP- and HRP-mediated reactions, respectively, using an ELISA reader (BioTek Instruments). A standard curve, using a serum with known concentrations of Igs, was run in parallel. Statistical analysis was performed using a two-way Student's *t* test.

Serum electrophoresis and immunofixation. Electrophoresis and immunofixation of human sera (*RAG*-mutated Omenn syndrome, $n = 4$; multiple myeloma, $n = 1$; systemic lupus erythematosus, $n = 1$; healthy control, $n = 1$) was performed according to the manufacturers instructions (HYDRASYS; Sebia, Inc.). Adjustments for mouse serum immunofixation were as follows: 20 μl of mouse serum and 15 μl of diluent (Sebia, Inc.) were mixed and 10 μl was loaded per lane (three lanes: protein electrophoresis/IgG/IgM). Donkey anti–mouse IgM and donkey anti–mouse IgG (Jackson ImmunoResearch Laboratories, Inc.) were diluted 1:5 in 0.9% NaCl. Theel was fixed using 38 μl ELP fixative (lane 1) or 24 μl of diluted anti–mouse IgG or anti–mouse IgM.

Determination of BAFF serum levels by ELISA. Evaluation of BAFF levels in mouse serum was performed by ELISA using a kit (R&D Systems) according to the manufacturer's instructions. Concentrations of BAFF in human sera were tested by ELISA as previously described (Lindh et al., 2008). Statistical analysis was performed using a two-tailed Student's *t* test.

Autoantibody detection. Levels of anti-ssDNA antibodies in mouse sera were assessed by ELISA, as previously described (Zouali and Stollar, 1986), with some modifications. In brief, Immulon (Dynatech Laboratories) plates were UV irradiated and then coated with 2.5 μg/ml ssDNA (Sigma-Aldrich). Samples were incubated on plates in 1:400 dilution, and then plates were washed and bound autoantibodies were detected with anti–mouse IgG- HRP (GE Healthcare), followed by incubation with TMB and reading at 450 nm. Levels of anti-ssDNA antibodies were expressed as ELISA units, using a standard curve prepared with serial dilutions of ANA-positive NZM2410 serum pool. For detection of light chain isotype of anti-ssDNA antibodies, final incubation was with anti–mouse κ or anti–mouse-λ AP antibody (SouthernBiotech), followed by reaction with p-NP and reading of OD at 405 nm. Results were expressed as the OD ratio (experimental OD/background OD).

Levels of anti-chromatin (anti-histone–DNA complex) antibodies in mouse sera were determined by ELISA as previously described (Mohan et al., 1998) and expressed as ELISA units, using a standard curve prepared with serial dilutions of ANA-positive NZM2410 serum pool, or expressed as OD ratio. For both anti-ssDNA and anti-chromatin antibodies, statistical analysis was performed using the Mann-Whitney *U* test.

For immunohistochemistry, Hep-2 cell–coated slides (Antibodies Incorporated) were incubated at room temperature with serum samples from *mut/mut* or +/+ mice at a 1:160 dilution, followed by incubation with Alexa Fluor 488 anti–mouse IgG F(ab′)$_2$ antibody (Invitrogen). Reactions were visualized by fluorescence microscopy. Background was adjusted with negative control samples. Slides were viewed with a microscope (Eclipse 90i; Nikon) using Plan Fluor 20× and Plan Apo 40x objectives (Nikon). Images were acquired using a camera (Orca-ER; Hamamatsu Photonics) and were processed with MetaMorph imaging software (version7.1.2.0; MDS Analytical Technologies). Statistical analysis was performed using the χ^2 test.

Affinity of serum anti-ssDNA antibodies was assessed in *mut/mut* ($n = 8$) and in NZM2410 ($n = 7$) mice by ELISA using increasing NaCl concentration. ELISA plates were prepared as previously described (Zouali and Stollar, 1986). Serum samples, diluted 1:400, were incubated at four different NaCl concentrations (150, 300, 600, and 1,200 mM). Plates were washed, and bound autoantibodies were detected with anti–mouse IgG-HRP (GE Healthcare), followed by incubation with TMB and reading at 450 nm. Levels of anti-ssDNA antibodies were expressed as percentage of OD compared with the OD_{max}, detected at physiological (150 mM NaCl) salt concentration. Statistical analysis was performed using two-way ANOVA.

Clinical data regarding tissue-specific autoantibodies from human subjects were obtained from collaborating sites. Human IgG/A/M ANAs were detected by immunohistochemistry, using slides coated with Hep-2 cells and cryostat tissues of rat kidney, liver, and stomach (Mosaik Basisprofil; Euroimmun), which were incubated at room temperature with patients' serum samples at 1:40 and 1:160 dilutions, followed by incubation with FITC–labeled anti-IgG/A/M conjugate (Euroimmun). Four samples from patients with *RAG* mutations that tested positive for ANA at a titer ≥1:80 were analyzed for ANA isotype, using FITC-conjugated anti–human IgG (BD) or FITC-conjugated anti–human IgM (BD). The reaction was visualized by fluorescence microscopy. Background was adjusted with negative control samples. Slides were viewed with a Leica DLMB microscope using HC PL Fluotar 20×/0.5 NA and HCX PL Fluotar 40×/0.75 NA objectives (Leica). Images were acquired using a camera (DFC 420C; Leica) and processed with Application Suite 3.4.0 imaging software (Leica). Statistical analysis was performed using the χ^2 test.

Online supplemental material. Fig. S1 shows oligoclonal repertoire of splenic B cells in *mut/mut* mice. Fig. S2 illustrates lack of germinal centers, and

abundance of extrafollicular ISCs, in the spleen of *mut/mut* mice. Fig. S3 depicts oligoclonality of serum Igs in *mut/mut* mice and in patients with Omenn syndrome. Fig. S4 shows that anti-ssDNA antibodies from *mut/mut* mice express κ light chain and show a variable pattern of cellular reactivity. Fig. S5 illustrates the presence of tissue-specific autoantibodies and glomerular deposits of IgM and C3 in *mut/mut* mice. Fig. S6 shows that adoptive transfer of wild-type $CD4^+$ T lymphocytes does not reduce levels of anti-chromatin antibodies in *mut/mut* mice. Fig. S7 depicts severity and composition of inflammatory infiltrates in various organs from *mut/mut* mice. Table S1 shows scoring of inflammatory infiltrates in *mut/mut* mice. Online supplemental material is available at http://www.jem.org/cgi/content/full/jem.20091927/DC1.

We thank Dr. Sergei Koralov (Immune Disease Institute, Harvard Medical School, Boston) for assisting with Vk-RS quantitative PCR, Attila Fabian for his assistance with sorting, Irina Gavanescu (Joslin Diabetes Center, Harvard Medical School, Boston) for reviewing tissue immunohistochemistry staining, Cristian Boboila (Immune Disease Institute, Harvard Medical School, Boston) for providing help for the ELISPOT assays, and Lisa Pitcher (Immune Disease Institute, Harvard Medical School, Boston) for assisting with kidney pathology immunofluorescence.

This work was partially contributed to by the National Institutes of Health Grants P01 AI076210-01A1 (to L.D. Notarangelo, F.W. Alt, and C. Terhorst), U54AI082973-01 (to M.J. Cowan, J.M. Puck, and L.D. Notarangelo) and AI063058 (to J. Sekiguchi), the 2008 Fellows Career Development Award by the American Academy of Allergy, Asthma and Immunology, American Thoracic Society and GlaxoSmithKline (to J.E. Walter), the Manton Foundation, the Dubai Harvard Foundation for Medical Research, the Jeffrey Model Diagnostic Center for Primary Immunodeficiencies at Children's Hospital Boston, Fondazione CARIPLO (to P.L. Poliani), and the University of California, San Francisco Jeffrey Model Diagnostic Center for Primary Immunodeficiencies. M. Recher was supported by grant PASMP3-127678/1 from the Swiss National Science Foundation (SNF/SSMBS).

The authors have no conflicting financial interests.

Submitted: 3 September 2009
Accepted: 18 May 2010

REFERENCES

Agenès, F., and A.A. Freitas. 1999. Transfer of small resting B cells into immunodeficient hosts results in the selection of a self-renewing activated B cell population. *J. Exp. Med.* 189:319–330. doi:10.1084/jem.189.2.319

Alt, F.W., and D. Baltimore. 1982. Joining of immunoglobulin heavy chain gene segments: implications from a chromosome with evidence of three D-JH fusions. *Proc. Natl. Acad. Sci. USA.* 79:4118–4122. doi:10.1073/pnas.79.13.4118

Brenchley, J.M., D.A. Price, T.W. Schacker, T.E. Asher, G. Silvestri, S. Rao, Z. Kazzaz, E. Bornstein, O. Lambotte, D. Altmann, et al. 2006. Microbial translocation is a cause of systemic immune activation in chronic HIV infection. *Nat. Med.* 12:1365–1371. doi:10.1038/nm1511

Cabatingan, M.S., M.R. Schmidt, R. Sen, and R.T. Woodland. 2002. Naive B lymphocytes undergo homeostatic proliferation in response to B cell deficit. *J. Immunol.* 169:6795–6805.

Cambridge, G., M.J. Leandro, M. Teodorescu, J. Manson, A. Rahman, D.A. Isenberg, and J.C. Edwards. 2006. B cell depletion therapy in systemic lupus erythematosus: effect on autoantibody and antimicrobial antibody profiles. *Arthritis Rheum.* 54:3612–3622. doi:10.1002/art.22211

Cao, W., L. Bover, M. Cho, X. Wen, S. Hanabuchi, M. Bao, D.B. Rosen, Y.H. Wang, J.L. Shaw, Q. Du, et al. 2009. Regulation of TLR7/9 responses in plasmacytoid dendritic cells by BST2 and ILT7 receptor interaction. *J. Exp. Med.* 206:1603–1614. doi:10.1084/jem.20090547

Carey, J.B., C.S. Moffatt-Blue, L.C. Watson, A.L. Gavin, and A.J. Feeney. 2008. Repertoire-based selection into the marginal zone compartment during B cell development. *J. Exp. Med.* 205:2043–2052. doi:10.1084/jem.20080559

Cariappa, A., M. Tang, C. Parng, E. Nebelitskiy, M. Carroll, K. Georgopoulos, and S. Pillai. 2001. The follicular versus marginal zone B lymphocyte cell fate decision is regulated by Aiolos, Btk, and CD21. *Immunity.* 14:603–615. doi:10.1016/S1074-7613(01)00135-2

Carneiro-Sampaio, M., and A. Coutinho. 2007. Tolerance and autoimmunity: lessons at the bedside of primary immunodeficiencies. *Adv. Immunol.* 95:51–82. doi:10.1016/S0065-2776(07)95002-6

Casellas, R., T.A. Shih, M. Kleinewietfeld, J. Rakonjac, D. Nemazee, K. Rajewsky, and M.C. Nussenzweig. 2001. Contribution of receptor editing to the antibody repertoire. *Science.* 291:1541–1544. doi:10.1126/science.1056600

Cassani, B., P.L. Poliani, V. Marrella, F. Schena, A.V. Sauer, M. Ravanini, D. Strina, C.E. Busse, S. Regenass, H. Wardemann, et al. 2010a. Homeostatic expansion of autoreactive immunoglobulin-secreting cells in the *Rag2* mouse model of Omenn syndrome. *J. Exp. Med.* 207:1525–1540.

Cassani, B., P.L. Poliani, D. Moratto, C. Sobacchi, V. Marrella, L. Imperatori, D. Vairo, A. Plebani, S. Giliani, P. Vezzoni, et al. 2010b. Defect of regulatory T cells in patients with Omenn syndrome. *J. Allergy Clin. Immunol.* 125:209–216. doi:10.1016/j.jaci.2009.10.023

Cavadini, P., W. Vermi, F. Facchetti, S. Fontana, S. Nagafuchi, E. Mazzolari, A. Sediva, V. Marrella, A. Villa, A. Fischer, et al. 2005. AIRE deficiency in thymus of 2 patients with Omenn syndrome. *J. Clin. Invest.* 115:728–732.

Chevrier, S., C. Genton, A. Kallies, A. Karnowski, L.A. Otten, B. Malissen, M. Malissen, M. Botto, L.M. Corcoran, S.L. Nutt, and H. Acha-Orbea. 2009. CD93 is required for maintenance of antibody secretion and persistence of plasma cells in the bone marrow niche. *Proc. Natl. Acad. Sci. USA.* 106:3895–3900. doi:10.1073/pnas.0809736106

Daitch, L.E., M.W. Moore, D.M. Persiani, J.M. Durdik, and E. Selsing. 1992. Transcription and recombination of the murine RS element. *J. Immunol.* 149:832–840.

Darce, J.R., B.K. Arendt, S.K. Chang, and D.F. Jelinek. 2007a. Divergent effects of BAFF on human memory B cell differentiation into Ig-secreting cells. *J. Immunol.* 178:5612–5622.

Darce, J.R., B.K. Arendt, X. Wu, and D.F. Jelinek. 2007b. Regulated expression of BAFF-binding receptors during human B cell differentiation. *J. Immunol.* 179:7276–7286.

de Villartay, J.P., A. Lim, H. Al-Mousa, S. Dupont, J. Déchanet-Merville, E. Coumau-Gatbois, M.L. Gougeon, A. Lemainque, C. Eidenschenk, E. Jouanguy, et al. 2005. A novel immunodeficiency associated with hypomorphic RAG1 mutations and CMV infection. *J. Clin. Invest.* 115:3291–3299. doi:10.1172/JCI25178

Durdik, J., M.W. Moore, and E. Selsing. 1984. Novel kappa light-chain gene rearrangements in mouse lambda light chain-producing B lymphocytes. *Nature.* 307:749–752. doi:10.1038/307749a0

Ehl, S., K. Schwarz, A. Enders, U. Duffner, U. Pannicke, J. Kühr, F. Mascart, A. Schmitt-Graeff, C. Niemeyer, and P. Fisch. 2005. A variant of SCID with specific immune responses and predominance of gamma delta T cells. *J. Clin. Invest.* 115:3140–3148. doi:10.1172/JCI25221

Gay, D., T. Saunders, S. Camper, and M. Weigert. 1993. Receptor editing: an approach by autoreactive B cells to escape tolerance. *J. Exp. Med.* 177:999–1008. doi:10.1084/jem.177.4.999

Giblin, W., M. Chatterji, G. Westfield, T. Masud, B. Theisen, H.L. Cheng, J. DeVido, F.W. Alt, D.O. Ferguson, D.G. Schatz, and J. Sekiguchi. 2009. Leaky severe combined immunodeficiency and aberrant DNA rearrangements due to a hypomorphic RAG1 mutation. *Blood.* 113:2965–2975. doi:10.1182/blood-2008-07-165167

Groom, J., S.L. Kalled, A.H. Cutler, C. Olson, S.A. Woodcock, P. Schneider, J. Tschopp, T.G. Cachero, M. Batten, J. Wheway, et al. 2002. Association of BAFF/BLyS overexpression and altered B cell differentiation with Sjögren's syndrome. *J. Clin. Invest.* 109:59–68.

Halverson, R., R.M. Torres, and R. Pelanda. 2004. Receptor editing is the main mechanism of B cell tolerance toward membrane antigens. *Nat. Immunol.* 5:645–650. doi:10.1038/ni1076

Hardy, R.R., C.E. Carmack, S.A. Shinton, J.D. Kemp, and K. Hayakawa. 1991. Resolution and characterization of pro-B and pre-pro-B cell stages in normal mouse bone marrow. *J. Exp. Med.* 173:1213–1225. doi:10.1084/jem.173.5.1213

Hayakawa, K., M. Asano, S.A. Shinton, M. Gui, D. Allman, C.L. Stewart, J. Silver, and R.R. Hardy. 1999. Positive selection of natural autoreactive B cells. *Science.* 285:113–116. doi:10.1126/science.285.5424.113

He, B., X. Qiao, and A. Cerutti. 2004. CpG DNA induces IgG class switch DNA recombination by activating human B cells through an innate

pathway that requires TLR9 and cooperates with IL-10. *J. Immunol.* 173:4479–4491.

Hondowicz, B.D., S.T. Alexander, W.J. Quinn III, A.J. Pagán, M.H. Metzgar, M.P. Cancro, and J. Erikson. 2007. The role of BLyS/BLyS receptors in anti-chromatin B cell regulation. *Int. Immunol.* 19:465–475. doi:10.1093/intimm/dxm011

Hsu, B.L., S.M. Harless, R.C. Lindsley, D.M. Hilbert, and M.P. Cancro. 2002. Cutting edge: BLyS enables survival of transitional and mature B cells through distinct mediators. *J. Immunol.* 168:5993–5996.

Kang, C.Y., T.K. Brunck, T. Kieber-Emmons, J.E. Blalock, and H. Kohler. 1988. Inhibition of self-binding antibodies (autobodies) by a VH-derived peptide. *Science.* 240:1034–1036. doi:10.1126/science.3368787

Khan, W.N., F.W. Alt, R.M. Gerstein, B.A. Malynn, I. Larsson, G. Rathbun, L. Davidson, S. Müller, A.B. Kantor, L.A. Herzenberg, et al. 1995. Defective B cell development and function in Btk-deficient mice. *Immunity.* 3:283–299. doi:10.1016/1074-7613(95)90114-0

Khiong, K., M. Murakami, C. Kitabayashi, N. Ueda, S. Sawa, A. Sakamoto, B.L. Kotzin, S.J. Rozzo, K. Ishihara, M. Verella-Garcia, et al. 2007. Homeostatically proliferating CD4 T cells are involved in the pathogenesis of an Omenn syndrome murine model. *J. Clin. Invest.* 117:1270–1281. doi:10.1172/JCI30513

Lavie, F., C. Miceli-Richard, M. Ittah, J. Sellam, J.E. Gottenberg, and X. Mariette. 2007. Increase of B cell-activating factor of the TNF family (BAFF) after rituximab treatment: insights into a new regulating system of BAFF production. *Ann. Rheum. Dis.* 66:700–703. doi:10.1136/ard.2006.060772

Lesley, R., Y. Xu, S.L. Kalled, D.M. Hess, S.R. Schwab, H.B. Shu, and J.G. Cyster. 2004. Reduced competitiveness of autoantigen-engaged B cells due to increased dependence on BAFF. *Immunity.* 20:441–453. doi:10.1016/S1074-7613(04)00079-2

Lindh, E., S.M. Lind, E. Lindmark, S. Hässler, J. Perheentupa, L. Peltonen, O. Winqvist, and M.C. Karlsson. 2008. AIRE regulates T-cell-independent B-cell responses through BAFF. *Proc. Natl. Acad. Sci. USA.* 105:18466–18471. doi:10.1073/pnas.0808205105

Liston, A., A. Enders, and O.M. Siggs. 2008. Unravelling the association of partial T-cell immunodeficiency and immune dysregulation. *Nat. Rev. Immunol.* 8:545–558. doi:10.1038/nri2336

Mackay, F., S.A. Woodcock, P. Lawton, C. Ambrose, M. Baetscher, P. Schneider, J. Tschopp, and J.L. Browning. 1999. Mice transgenic for BAFF develop lymphocytic disorders along with autoimmune manifestations. *J. Exp. Med.* 190:1697–1710. doi:10.1084/jem.190.11.1697

Marrella, V., P.L. Poliani, A. Casati, F. Rucci, L. Frascoli, M.L. Gougeon, B. Lemercier, M. Bosticardo, M. Ravanini, M. Battaglia, et al. 2007. A hypomorphic R229Q Rag2 mouse mutant recapitulates human Omenn syndrome. *J. Clin. Invest.* 117:1260–1269. doi:10.1172/JCI30928

Mayne, C.G., I.J. Amanna, F.E. Nashold, and C.E. Hayes. 2008. Systemic autoimmunity in BAFF-R-mutant A/WySnJ strain mice. *Eur. J. Immunol.* 38:587–598. doi:10.1002/eji.200737817

Melchers, F. 2006. Anergic B cells caught in the act. *Immunity.* 25:864–867. doi:10.1016/j.immuni.2006.11.003

Merrell, K.T., R.J. Benschop, S.B. Gauld, K. Aviszus, D. Decote-Ricardo, L.J. Wysocki, and J.C. Cambier. 2006. Identification of anergic B cells within a wild-type repertoire. *Immunity.* 25:953–962. doi:10.1016/j.immuni.2006.10.017

Meyer-Bahlburg, A., S.F. Andrews, K.O. Yu, S.A. Porcelli, and D.J. Rawlings. 2008. Characterization of a late transitional B cell population highly sensitive to BAFF-mediated homeostatic proliferation. *J. Exp. Med.* 205:155–168. doi:10.1084/jem.20071088

Miller, J.P., J.E. Stadanlick, and M.P. Cancro. 2006. Space, selection, and surveillance: setting boundaries with BLyS. *J. Immunol.* 176:6405–6410.

Mohan, C., E. Alas, L. Morel, P. Yang, and E.K. Wakeland. 1998. Genetic dissection of SLE pathogenesis. Sle1 on murine chromosome 1 leads to a selective loss of tolerance to H2A/H2B/DNA subnucleosomes. *J. Clin. Invest.* 101:1362–1372.

Moisini, I., and A. Davidson. 2009. BAFF: a local and systemic target in autoimmune diseases. *Clin. Exp. Immunol.* 158:155–163. doi:10.1111/j.1365-2249.2009.04007.x

Muramatsu, M., K. Kinoshita, S. Fagarasan, S. Yamada, Y. Shinkai, and T. Honjo. 2000. Class switch recombination and hypermutation require activation-induced cytidine deaminase (AID), a potential RNA editing enzyme. *Cell.* 102:553–563. doi:10.1016/S0092-8674(00)00078-7

Negishi, I., N. Motoyama, K. Nakayama, K. Nakayama, S. Senju, S. Hatakeyama, Q. Zhang, A.C. Chan, and D.Y. Loh. 1995. Essential role for ZAP-70 in both positive and negative selection of thymocytes. *Nature.* 376:435–438. doi:10.1038/376435a0

Nijnik, A., S. Dawson, T.L. Crockford, L. Woodbine, S. Visetnoi, S. Bennett, M. Jones, G.D. Turner, P.A. Jeggo, C.C. Goodnow, and R.J. Cornall. 2009. Impaired lymphocyte development and antibody class switching and increased malignancy in a murine model of DNA ligase IV syndrome. *J. Clin. Invest.* 119:1696–1705. doi:10.1172/JCI32743

Ochs, H.D., S.D. Davis, E. Mickelson, K.G. Lerner, and R.J. Wedgwood. 1974. Combined immunodeficiency and reticuloendotheliosis with eosinophilia. *J. Pediatr.* 85:463–465. doi:10.1016/S0022-3476(74)80445-2

Oettinger, M.A., D.G. Schatz, C. Gorka, and D. Baltimore. 1990. RAG-1 and RAG-2, adjacent genes that synergistically activate V(D)J recombination. *Science.* 248:1517–1523. doi:10.1126/science.2360047

Panigrahi, A.K., N.G. Goodman, R.A. Eisenberg, M.R. Rickels, A. Naji, and E.T. Luning Prak. 2008. RS rearrangement frequency as a marker of receptor editing in lupus and type 1 diabetes. *J. Exp. Med.* 205:2985–2994. doi:10.1084/jem.20082053

Pessach, I., J. Walter, and L.D. Notarangelo. 2009. Recent advances in primary immunodeficiencies: identification of novel genetic defects and unanticipated phenotypes. *Pediatr. Res.* 65:3R–12R. doi:10.1203/PDR.0b013e31819dbe1e

Pillai, S., A. Cariappa, and S.T. Moran. 2004. Positive selection and lineage commitment during peripheral B-lymphocyte development. *Immunol. Rev.* 197:206–218. doi:10.1111/j.0105-2896.2003.097.x

Poliani, P.L., F. Facchetti, M. Ravanini, A.R. Gennery, A. Villa, C.M. Roifman, and L.D. Notarangelo. 2009. Early defects in human T-cell development severely affect distribution and maturation of thymic stromal cells: possible implications for the pathophysiology of Omenn syndrome. *Blood.* 114:105–108. doi:10.1182/blood-2009-03-211029

Radic, M.Z., J. Erikson, S. Litwin, and M. Weigert. 1993. B lymphocytes may escape tolerance by revising their antigen receptors. *J. Exp. Med.* 177:1165–1173. doi:10.1084/jem.177.4.1165

Reimold, A.M., N.N. Iwakoshi, J. Manis, P. Vallabhajosyula, E. Szomolanyi-Tsuda, E.M. Gravallese, D. Friend, M.J. Grusby, F. Alt, and L.H. Glimcher. 2001. Plasma cell differentiation requires the transcription factor XBP-1. *Nature.* 412:300–307. doi:10.1038/35085509

Retter, M.W., and D. Nemazee. 1998. Receptor editing occurs frequently during normal B cell development. *J. Exp. Med.* 188:1231–1238. doi:10.1084/jem.188.7.1231

Rucci, F., L.D. Notarangelo, A. Fazeli, L. Patrizi, T. Hickernell, T. Paganini, K.M. Coakley, C. Detre, M. Keszei, J.E. Walter, et al. 2010. Homozygous DNA ligase IV R278H mutation in mice leads to leaky SCID and represents a model for human LIG4 syndrome. *Proc. Natl. Acad. Sci. USA.* 107:3024–3029. doi:10.1073/pnas.0914865107

Schatz, D.G., M.A. Oettinger, and D. Baltimore. 1989. The V(D)J recombination activating gene, RAG-1. *Cell.* 59:1035–1048. doi:10.1016/0092-8674(89)90760-5

Scheiffele, F., and I.J. Fuss. 2002. Induction of TNBS colitis in mice. *Curr. Protoc. Immunol.* Chapter 15:15: 19.

Schuetz, C., K. Huck, S. Gudowius, M. Megahed, O. Feyen, B. Hubner, D.T. Schneider, B. Manfras, U. Pannicke, R. Willemze, et al. 2008. An immunodeficiency disease with RAG mutations and granulomas. *N. Engl. J. Med.* 358:2030–2038. doi:10.1056/NEJMoa073966

Schwarz, K., G.H. Gauss, L. Ludwig, U. Pannicke, Z. Li, D. Lindner, W. Friedrich, R.A. Seger, T.E. Hansen-Hagge, S. Desiderio, et al. 1996. RAG mutations in human B cell-negative SCID. *Science.* 274:97–99. doi:10.1126/science.274.5284.97

Signorini, S., L. Imberti, S. Pirovano, A. Villa, F. Facchetti, M. Ungari, F. Bozzi, A. Albertini, A.G. Ugazio, P. Vezzoni, and L.D. Notarangelo. 1999. Intrathymic restriction and peripheral expansion of the T-cell repertoire in Omenn syndrome. *Blood.* 94:3468–3478.

Sobacchi, C., V. Marrella, F. Rucci, P. Vezzoni, and A. Villa. 2006. RAG-dependent primary immunodeficiencies. *Hum. Mutat.* 27:1174–1184. doi:10.1002/humu.20408

Stadanlick, J.E., and M.P. Cancro. 2008. BAFF and the plasticity of peripheral B cell tolerance. *Curr. Opin. Immunol.* 20:158–161. doi:10.1016/j.coi.2008.03.015

Thien, M., T.G. Phan, S. Gardam, M. Amesbury, A. Basten, F. Mackay, and R. Brink. 2004. Excess BAFF rescues self-reactive B cells from peripheral deletion and allows them to enter forbidden follicular and marginal zone niches. *Immunity.* 20:785–798. doi:10.1016/j.immuni.2004.05.010

Tiegs, S.L., D.M. Russell, and D. Nemazee. 1993. Receptor editing in self-reactive bone marrow B cells. *J. Exp. Med.* 177:1009–1020. doi:10.1084/jem.177.4.1009

Tsai, C.L., A.H. Drejer, and D.G. Schatz. 2002. Evidence of a critical architectural function for the RAG proteins in end processing, protection, and joining in V(D)J recombination. *Genes Dev.* 16:1934–1949. doi:10.1101/gad.984502

Tsitsikov, E.N., J.C. Gutierrez-Ramos, and R.S. Geha. 1997. Impaired CD19 expression and signaling, enhanced antibody response to type II T independent antigen and reduction of B-1 cells in CD81-deficient mice. *Proc. Natl. Acad. Sci. USA.* 94:10844–10849. doi:10.1073/pnas.94.20.10844

Ueda, Y., D. Liao, K. Yang, A. Patel, and G. Kelsoe. 2007. T-independent activation-induced cytidine deaminase expression, class-switch recombination, and antibody production by immature/transitional 1 B cells. *J. Immunol.* 178:3593–3601.

Vela, J.L., D. Aït-Azzouzene, B.H. Duong, T. Ota, and D. Nemazee. 2008. Rearrangement of mouse immunoglobulin kappa deleting element recombining sequence promotes immune tolerance and lambda B cell production. *Immunity.* 28:161–170. doi:10.1016/j.immuni.2007.12.011

Villa, A., S. Santagata, F. Bozzi, S. Giliani, A. Frattini, L. Imberti, L.B. Gatta, H.D. Ochs, K. Schwarz, L.D. Notarangelo, et al. 1998. Partial V(D)J recombination activity leads to Omenn syndrome. *Cell.* 93:885–896. doi:10.1016/S0092-8674(00)81448-8

Villa, A., C. Sobacchi, L.D. Notarangelo, F. Bozzi, M. Abinun, T.G. Abrahamsen, P.D. Arkwright, M. Baniyash, E.G. Brooks, M.E. Conley, et al. 2001. V(D)J recombination defects in lymphocytes due to RAG mutations: severe immunodeficiency with a spectrum of clinical presentations. *Blood.* 97:81–88. doi:10.1182/blood.V97.1.81

Wardemann, H., S. Yurasov, A. Schaefer, J.W. Young, E. Meffre, and M.C. Nussenzweig. 2003. Predominant autoantibody production by early human B cell precursors. *Science.* 301:1374–1377. doi:10.1126/science.1086907

Wardemann, H., J. Hammersen, and M.C. Nussenzweig. 2004. Human autoantibody silencing by immunoglobulin light chains. *J. Exp. Med.* 200:191–199. doi:10.1084/jem.20040818

Zekavat, G., S.Y. Rostami, A. Badkerhanian, R.F. Parsons, B. Koeberlein, M. Yu, C.D. Ward, T.S. Migone, L. Yu, G.S. Eisenbarth, et al. 2008. In vivo BLyS/BAFF neutralization ameliorates islet-directed autoimmunity in nonobese diabetic mice. *J. Immunol.* 181:8133–8144.

Zouali, M., and B.D. Stollar. 1986. A rapid ELISA for measurement of antibodies to nucleic acid antigens using UV-treated polystyrene microplates. *J. Immunol. Methods.* 90:105–110. doi:10.1016/0022-1759(86)90390-X